Machine Learning-supported MRI Analysis of Brain Asymmetry for Early Diagnosis of Dementia

Nitsa J. Herzog and George D. Magoulas

Abstract The chapter focuses on the detection of early degenerative processes in the human brain using computational algorithms and machine learning classification techniques. The research is consistent with the hypothesis that there are changes in brain asymmetry across stages of dementia and Alzheimer's Disease. The proposed approach considers the pattern of changes in the degree of asymmetry between the left and right hemispheres of the brain using structural magnetic resonance imaging of the ADNI database and image analysis techniques. An analysis of levels of asymmetry is performed with the help of statistical features extracted from the segmented asymmetry images. The diagnostic potential of these features is explored using variants of Support Vector Machines and a Convolutional Neural Network. The proposed approach produces very promising results in distinguishing between cognitively normal subjects and patients with early mild cognitive impairment and Alzheimer's Disease, providing evidence that image asymmetry features or MRI images of segmented asymmetry can offer insight on early diagnosis of dementia.

Nitsa J. Herzog [1] and George D. Magoulas[2]

[1] Department of Computer Science, Birkbeck College, University of London, WC1E 7HZ, UK; nitsa@dcs.bbk.ac.uk

[2] Birkbeck Knowledge Lab, University of London, WC1E 7HZ, UK; g.magoulas@bbk.ac.uk

1 Introduction

The human brain is examined with a help of advanced modern technology, which provides detailed scans of the brain tissues and demonstrates the functional activity of the brain regions associated with a specific mental or behavioural task.

Brain scanning is divided into two large categories: structural imaging and functional imaging. The most common structural neuroimaging methods are X-ray, structural Magnetic Resonance Imaging (sMRI), Diffusion Tensor Imaging (DTI), modification of MRI, and Computerized Tomography (CT) (Kimberley and Lewis 2007). Well-known functional methods are Electroencephalography (EEG), functional Magnetic Resonance Imaging (fMRI), and Positron Emission Tomography (PET) (Bunge and Kahn 2009). MRI covers around 50% of imaging data used for the diagnosis of brain diseases (Segato et al. 2020). A significant advantage of MRI over popular CT and X-ray scans is the absence of ionizing radiation during the MRI session. The MRI contrasting agent is less allergic than iodine-based substances of CT scans and X-rays. Another advantage of MRI is the possibility to provide a high level of soft-tissue contrast resolution compared to a CT scan, which is superior at imaging hard anatomical structures. All these factors make MRI the method of choice for regular health checks in the population older than 60. High-resolution images make a significant impact on the computer-aided diagnosis of brain-related disorders.

Early dementia, or amnestic Mild Cognitive Impairment (aMCI), belongs to the group of neurocognitive disorders and is characterized by some sort of short-time memory loss, language difficulties, lack of reasoning and judgment, hardship coping with daily routines (Janelidze and Botchorishvili 2018). Approximately 10% of the world population, aged between 70 and 79, and 25% of the population older than 80, are diagnosed with MCI. It is acknowledged that 80% of the patients with aMCI develop severe dementia, in the form of Alzheimer's disease, within 7 years. The proportion of dementia in the general population is 7.1 %, which is roughly 46.8 million people.

Neurogenerative disorders, such as Alzheimer's disease (AD), which is the most common, followed by vascular dementia, Lewy body dementia, Frontotemporal dementia, Parkinson's disease and Huntington's disease, severely affect memory and other mental tasks (Agarwal et al., 2021). As amnestic MCI often becomes a prodrome of Alzheimer's disease, it is important to identify this form of dementia in the early stage when proper care and treatment can stop or slow down the progression of the disease.

The diagnosis of MCI is based on neuropsychological testing, blood testing, and neuroimaging (ICD-11 2018; DSM-V 2013). Mini-Mental State Examination (MMSE), Montreal Cognitive Assessment (MoCA), and Geriatric Mental State

Examination (GMS) are the most common cognitive screening assessments. The tests usually include groups of questions assessing orientation in place and time, short-time memory, attention, recall, and language ability of coherent speaking and understanding. For clinical judgment between MCI and AD certain types of biomarkers, measured in the cerebrospinal fluid (CSF), are used. Amyloid-beta 42 (Ab42), total tau (T-tau), and phosphorylated tau (P-tau) globulins are identified in the early stage of Alzheimer's disease, whilst Hippocampal volume and rate of brain atrophy finalize the diagnosis.

The research presented in this chapter is focused on the early detection and classification of dementia using sMRI, when changes in the brain are not obvious for radiologists or clinical practitioners, the amyloid-beta deposition may be present or not, and the tau globulin is absent. This work involves the segmentation and evaluation of asymmetries in the cortex of the brain and the classification of dementia using machine learning algorithms.

2 Literature review

The two brain hemispheres have slightly different anatomy and function, and a detailed examination of their structure shows a variety of asymmetrical areas. The revealed lateralization originates from genetic and epigenetic factors in the evolutionary development of the human brain (Isles 2018). The exposure of the pathological factors during a human life also might cause changes in the lateralization of the brain.

The evolutionary expansion of the left-hemispheric area is closely connected to speech production, perception, and motor dominance. The earliest observations of brain asymmetry were reported by the French physician, anatomist and anthropologist Pierre Paul Broca in the 19th century, and then, 10 years later by German neurologist Carl Wernicke. They found that the language of the patient was severely impaired when a stroke or tumor had affected the left-brain hemisphere. Broca localized the afflicted area in the anterior left hemisphere, including some parts of the inferior frontal gyrus (the so-called "Broca's area"). The pathological process in that area of the brain significantly changed the language production and syntactic processing of the patients. Changes in language comprehension, such as understanding spoken words, were primarily discovered by Wernicke in the posterior temporal-parietal region (the so-called "Wernicke's area"). Thus, it was confirmed that differences in the anatomical structure of the brain correlate with their functional lateralization. The left hemisphere is mostly responsible for language processing and logical thinking. The right hemisphere specializes in spatial recog-

nition, attention, musical and artistic abilities. Emotions and their manifestation are also connected to the right hemisphere (Gainotti 2019).

Brain asymmetry is closely related to human handedness. An interesting fact is that the foetal orientation during the pregnancy is correlated with the handedness of a newborn child. These asymmetries are first observed in the 29-31 weeks of gestational age. Almost 90% of the human population is right-handed (McManus 2019). "Petalia and Yakovlevian torque" (Segato et al. 2020) is a term that describes an overall leftward posterior and rightward anterior asymmetry usually presented in right-handed individuals. Around 95% of right-handed persons have their speech and language zones in the left hemisphere, while only 5% show the language zone representation in the right hemisphere or bilateral. Compared to the right-handed people, the left-handed demonstrate a higher ratio of hemispheric lateralization. A strongly dominant right hemisphere lateralization presents only in 7% of left-handers. This proportion can vary with age. Up to 85% of left-handed children have language area dominance in the left hemisphere (Szaflarski et al. 2012).

Some studies highlight the differences in hemispheric lateralization between males and females (Tomasi and Volkow 2012). The distinctions can be noticeable in linguistic performance, visuospatial or motor skills. The female brains show more symmetries in both cerebral hemispheres.

The level of asymmetry also depends on the age of the person. The brain functional hemispheric asymmetry in the frontal lobes of young adults is more lateralized than in elderly healthy persons. The activity reduction of the frontal cortex leads to age-related cognitive decline. It is registered by functional neuroimaging as changes in the domains of semantic, episodic, or working memory, perception, and inhibitory control. Elderly people demonstrate compensatory processes in the brain that transform brain lateralization. Sometimes it looks like bilateral hemispheric activity (Cabeza et al. 2004).

2.1 Brain asymmetry for the diagnosis of brain-related disorders

The brain regions show a progressive decrease in the degree of asymmetry in patients with Mild Cognitive Impairment (MCI) and an increase of asymmetry in patients with Alzheimer's disease (AD) (Yang et al. 2017). To prove this concept Yang et al. used diffusion tensor image tractography to construct the hemispheric brain white matter networks. The researchers concluded that the brain white matter (WM) networks show the rightward topological asymmetry, when the right cerebral hemisphere becomes dominant in AD patients, but not in the early phase

of the MCI. Left-hemisphere regions are affected earlier and more severely. The abnormal hemispheric asymmetry of AD and MCI patients significantly correlates with memory performance.

The functional cortical asymmetry progressively decreases in patients with MCI (Liu et al. 2018). Liu et al.'s research was based on whole-brain imaging. They registered and compared the spontaneous brain activity in patients with MCI, AD and NC (normal controls) using functional MRI. They discovered that patients with MCI and AD have abnormal rightward laterality in the brain compared to healthy controls with observed leftward lateralization. At the same time alterations in the brain lateralization between patients with MCI and normal controls were different from alteration between patients with AD and normal controls. The rightward lateralization in the patients with MCI and AD may be reflected as a relative increase in brain activation within the right hemisphere or a relative decrease in brain activation within the left hemisphere. Patients with MCI showed an increase in the activation of several brain regions in the right hemisphere during the processing of word memory tasks. Those areas were compensatorily activated compared to the activation zones in the left hemisphere of the healthy controls. Liu et al. suppose that the reason for the abnormal right-lateralized pattern in patients with AD might be more complex than in patients with MCI. They think that functional results are potentially influenced by structural differences between the groups, but they did not investigate the relationship between brain structural asymmetry and brain functional lateralization in their research. All participants in the study were right-handed. The researchers did not determine whether the same right brain lateralization occurs in left-handed persons. They found a significant difference in brain functionality between MCI and AD patients. The patients with MCI had normal leftward lateralization with some elements of abnormal rightward activity. In patients with AD, the normal pattern of left lateralization disappeared, and some abnormal right-lateralized pattern was detected.

The degree of asymmetry is not the same in the different parts of the brain (Kim et al. 2012). Kim et al. tested the hypothesis that individuals with aMCI and different stages of AD have reductions of asymmetries in the heteromodal neocortex. They found significant changes in the degree of asymmetry in the inferior parietal lobe of the brain of right-handed adults. The cortical asymmetry was investigated using surface-based morphometry (SBM) to measure the cortical thickness. Their results show that the neocortical thickness asymmetries of the medial and lateral sides of the right and left parts of the brain were different from each other. The decrease of asymmetry was registered in the lateral parts of the frontal and parietal lobes and there was an increase in the temporal lobe. The left perisylvian areas responsible for language functions, except Broca's speech area, demonstrated leftward asymmetry. Other areas of the brain, which specialized in spatial percep-

tion, facial recognition, and memory processing, showed rightward asymmetry. Kim et al. assumed that the cortical asymmetry shown in healthy controls generally decreases in AD. However, they did not directly examine the changes in cortical asymmetry observed during the AD progression, which gives a clear picture of an increase in asymmetry in the case of severe AD. Also, it is unclear whether similar changes in cortical asymmetry can be caused by other degenerative diseases.

Wachinger et al. investigated the neurodegenerative processes in the subcortical brain structures of patients with AD (Wachinger et al. 2016). They proposed a measure of brain asymmetry which is based on spectral shape descriptors from the BrainPrint. BrainPrint is an ensemble of shape descriptors that represents brain morphology and captures shape information of cortical and subcortical structures. Progressive dementia is associated with a significant increase in the neuroanatomical asymmetry in the hippocampus and amygdala. The research findings (see Table 1 for an overview) prove that shape analysis can detect the progression of dementia earlier than volumetric measures. Shape asymmetry, based on longitudinal asymmetry measures in the hippocampus, amygdala, caudate and cortex can be a powerful imaging biomarker for the early presymptomatic prediction of dementia.

Table 1. State-of-the-art neuroscientific methods of registration of brain asymmetry

Reference	Method	Conclusion
Yang et al. (2017)	Diffusion tensor image (DTI) tractography to construct the hemispheric brain white matter networks	Decrease of asymmetry in patients with MCI and an increase of asymmetry in patients with AD
Liu et al. (2018)	Registration of the spontaneous brain activity in patients with MCI, AD and NC using functional MRI (fMRI)	The functional cortical asymmetry progressively decreases in patients with MCI
Kim et al. (2012)	Surface-based morphometry (SBM) to measure cortical thickness	The degree of asymmetry is not the same in the different parts of the brain
Wachinger et al. (2016)	Measurement of brain asymmetry based on spectral shape descriptors using BrainPrint	Progressive dementia is associated with an increase in asymmetry in the hippocampus and amygdala; shape analysis can detect the progression of dementia earlier than volumetric measures

2.2 Classification of Alzheimer's Disease and early mild cognitive impairment using the ADNI database

The Alzheimer's Disease Neuroimaging Initiative (ADNI) database (adni.loni.usc.edu) was launched in 2003 as a public-private partnership led by Michael W. Weiner, MD. The primary goal of ADNI has been to test whether serial magnetic resonance imaging (MRI), positron emission tomography (PET), other biological markers, and clinical and neuropsychological assessment can be combined to measure the progression of mild cognitive impairment (MCI) and early Alzheimer's disease (AD) (for up-to-date information, see www.adni-info.org). Multiple research studies have benefited from MRI data of the ADNI database. The rest of this section focuses on machine learning approaches for the modelling and classification of neurogenerative disease, including mild cognitive impairment and Alzheimer's Disease, stable and progressive forms of MCI, as these are more relevant to this work.

A large portion of research in this area consists of machine learning-based diagnostic approaches that use features engineering as this has been shown to contribute towards successful modelling. For example, Beheshti et al. (2017) implemented feature-ranking and a genetic algorithm to analyze structural magnetic resonance imaging data of 458 subjects. The researchers state that the proposed system can distinguish between stable and progressive MCI and to predict the conversion of MCI to Alzheimer's Disease from one to three years ahead it will be clinically diagnosed. Beheshti et al. (2017) identified atrophic gray matter (GM) regions using voxel-based morphometry (VBM). The features were extracted after applying a 3D mask and they were ranked according to their t-test scores. Features with t-test values higher than 70% were combined into new subsets. A genetic algorithm, with the Fisher criterion function (Welling 2005), evaluated the separation between the two groups of data and helped to select the most discriminative feature subsets for the classification. The classification process was finalized with linear SVM (Evgeniou and Pontil 1999), and classification performance was evaluated with a 10-fold cross-validation procedure. The calculated accuracy shows 93.01% for stable MCI and 75% for progressive MCI. The feature selection process raised the accuracy from 78.94% to 94.73%.

Another group of scientists (Moradi et al. 2015) investigated the conversion of MCI to AD. Their algorithm identifies AD in a period between one to three years prior to the development of clinical symptoms. The proposed algorithm is based on aggregated biomarkers and a random forest (RF) classifier (Breiman 2001). The MRI data were preprocessed by removing images with age-related changes in the anatomical structure of the brain using a linear regression model. Feature se-

lection was implemented on AD and NC images by a regularized logistic regression (RLG) algorithm (Tripepi 2008). The classification stage is performed using a semi-supervised low-density separation (LDS) method (the LDS is a two steps algorithm, which relies on the graph-distance kernel and the Transductive Support Vector Machine-TSVM learning). At the beginning of this stage, the classifier is trained with labelled AD and NC data. Then, unlabeled MCI images are fed into the classifier. It helps to separate the stable and progressive MCI and get them labelled. In the final stage the output of the LDS classifier, as an input feature, is combined with age and cognitive measurements feature vectors into the RF classifier. The aggregated biomarker distinguishes between stable and progressive MCI and approximates the probability of conversion of MCI to AD. The testing of image sequences of 825 subjects was done with a 10-fold cross-validation method. The results showed that the predictive performance of the aggregated biomarker is higher than the performance of single biomarkers. MRI data with a combination of cognitive and age measures improves the classification accuracy by 5.5% (from 76.5% to 82%).

Another approach, (Zhu et al. 2017), proposed an algorithm for the Joint Regression and Classification (JRC) problem in the diagnosis of MCI and AD. The idea behind this regularization-based method is to consider the related similarity of features, samples, and their responses. The features are related to each other if their respective weight coefficients are similar. The weight coefficients are linked to the response variables via feature vectors and demonstrate the resembling type of relation. The same rule is applied to a similar pair of samples and their respective response values. The regularization method was tested with MRI and PET (Positron Emission Tomography) image sequences of 202 subjects (Wong et al.2003). The images were separated into 93 regions of interest (ROI) using a volumetric measure of the gray matter of the brain. Structural MRI scans were aligned with functional PET images using affine registration. The average intensity values were calculated for each ROI. Structurally and functionally related to each other features were extracted from each ROI and sent to the feature selection process using the regularization algorithm. Extracted features were expected to predict jointly one clinical label and two clinical scores. Imaging data for clinical labelling were classified with SVM. Other types of data obtained from cognitive tests were used for training two more Support Vector Regression (SVR) models for prediction of clinical scores of AD Assessment Scale-Cognitive Subscale (ADAS-Cog) and Mini-Mental State Examination (MMSE) (Nogueira et al. 2018). The results were obtained using binary classification methods and 10-fold cross-validation. In the initial stage of the experiment, the classification and regression tasks were performed without feature selection. The results of this stage were considered as a baseline. In the next run, the baseline was compared to sin-

gle-task results, when the selected features are classified independently, and multi-task results when the features are classified jointly for the classification and regression models. The proposed joint approach shows the superiority of the single-task approach by 5.6%. Compared to the baseline, the average accuracy for a single task increases by 6%, and for multi-task by 8.8%. The proposed models were compared with two state-of-the-art methods: High-Order Graph Matching (HOGM) (Duchenne et al. 2011) and Multi-Modal Multi-Task (M3T) (Zhang and Shen 2011). The Joint Regression and Classification model outperform their competitors by improving classification accuracy by 5% (vs. HOGM) and 4.7% (vs. M3T) for MRI, and 4.6% (vs. HOGM) and 4.2% (vs. M3T) for PET. The highest archived accuracy for classification AD vs NC is 95.7%, MCI vs NC is 79.9%.

Another stream of research is taking advantage of machine learning methods that generate features as part of the training process. These methods employ Artificial Neural Networks and Deep Learning and have attracted a lot of attention in the area of medical image analysis and classification recently. They can process a large amount of data and learn in a supervised (labelled) or unsupervised (unlabelled) mode. Particularly, diagnostic approaches that use Deep Learning in most cases do not require complicated, time-consuming image preprocessing and feature engineering techniques and produce state-of-the-art results.

In this setting, the Convolutional Neural Network (CNN) is one of the models successfully adapted to classify imaging data (Yamashita et al. 2018). Basaia et al. (2019) built and evaluated a CNN algorithm that predicts AD, progressive cognitive mild impairment, and stable cognitive impairment. The architecture of the network included 12 repeated blocks of convolutional layers, an activation layer, a fully-connected layer, and one logistic regression output layer. The researchers used T1-waited structural MRIs of 1409 subjects from the ADNI database. The image data was split into training, validation, and testing sets in the proportion of 90% for the first two, and 10% for the last one. 10-fold cross-validation was applied. Weights of the CNN used for classification of AD vs HC dataset were applied as pre-trained initial weights to the other CNNs. This technique reduced the training time and increase the network performance. High predictive accuracy was achieved in both databases with no significant difference. The highest percentage for AD vs HC (healthy control) classification accuracy was: 99% for ADNI. For c-MCI vs HC, and s-MCI vs HC accuracy was 87% and 76% respectively, while for AD vs c-MCI and AD vs s-MCI performance was 75% and 86%, and for c-MCI vs s-MCI 75%.

Multi-Layer Perceptron and a Convolutional Bidirectional Long Short-Term Memory (ConvBLSTM) model were proposed by Stamate et al. in the diagnosis of dementia (Stamate et al. 2020). Different clinical sources and protocols of 1851 participants of the ADNI database were combined. The collected bi-

omarkers consist of 51 input attributes and include baselines demographics data, functional activity questionnaire, Mini-Mental State Exam (MMSE), cerebrospinal fluid (CSF) biomarkers, neuropsychological tests, and measurements received from MRI, RET and genetic data. The ReliefF method (Robnik-Šikonja and Kononenko 2003) and permutation test (Pesarin and Salmaso 2010), including 500 permutations of labels, were combined for feature selection and ranking. The top-10 ranked features have been sent to classification models. 75 % of the data were used for training and the rest for testing. The predictive results were obtained using Monte Carlo simulations (Johansen et al. 2010). All models were able to accurately predict dementia and mild cognitive impairment. The highest accuracy of 86% was achieved with the Multi-Layer Perceptron model.

Lastly, another study (Lama et al. 2017) proposed an unsupervised deep learning method for the classification of AD, MCI, and NC. The algorithm extracts the features with PCA (Abdi and Williams 2010) and processes them with a Regularized Extreme Learning Machine (RELM) (Ding et al. 2014). RELM is based on single hidden-layer feedforward neural network. The investigators chose high-level features using the Softmax function (a function that takes a vector of real numbers as input and normalizes it into a probability distribution). The results of RELM are compared with multiple kernel SVM and import vector machine (IVM) (IVM classifier based on Kernel Logic Regression uses a few data points to define the decision hyperplane and has a probabilistic output). The researchers have done 100 tests of imaging data collected from 214 subjects using 10-fold cross-validation and 10 tests with the leave-one-out method. They separated training and testing images with a ratio of 70/30 for the 10-fold cross-validation, and 90/10 for the leave-one-out validation. The study confirmed that RELM improves the classification accuracy of AD and MCI from 75.33% to 80.32% for binary classification and 76.61% for multiclass classification.

The above approaches are summarized in Table 2.

Table 2 Methods of diagnosis of Mild Cognitive Impairment and Alzheimer's Disease, used in the literature

Reference	Modality	Classification type	Method	Complexity	Best result
Beheshti et al. (2017)	sMRI	Linear SVM	Feature ranking and genetic algorithm	Medium	Stable MCI 93.01%, progressive MCI 75%
Moradi et al. (2015)	Aggregated biomarkers (MRI + age + cognitive measures)	Semi-supervised low-density separation (LDS) + Random Forest (RF)	Feature selection from MRI with LDS, final result obtained with RF	High	Progressive MCI 82%
Zhu et al. (2017)	sMRI, PET, cognitive measures	Joint regression and classification (SVM)	Alignment of structural and functional features, feature selection with regularization algorithm	High	AD vs NC 95.7%, MCI vs NC 79.9%
Basaia et al. (2019)	sMRI	CNN	Pretrained CNN	Low	AD vs. NC 98%, sMCI vs. cMCI 75%
Stamate et al. (2020)	51 aggregated biomarkers without imaging data	Multi-Layer Perceptron and a Convolutional Bidirectional Long Short-Term Memory (ConvBLSTM) model	Feature selection and ranking, top 10 features are used with NN models	Medium	Dem vs MCI vs CN 86%
Lama et al. (2017)	sMRI	Unsupervised DL (Regularized Extreme Learning Machine (RELM))	Features extracted with PCA and process with RELM	Medium	AD vs MCI vs NC 76.61%, AD vs MCI 80.32%

3 The proposed approach

The machine learning workflow for early diagnosis of dementia (Fig. 1) includes image preprocessing, segmentation of image asymmetries, extraction of statistical features and image analysis, and machine learning classification algorithms. The visualized differences between the right and the left hemispheres of the MRI slices of the brain are used for features extraction. This simplifies the feature engineering stage because the collected features are already selected from the brain regions affected by degenerative processes. The images of segmented asymmetries require less storage than original MRIs. This speed up the classification processing of large datasets using images as an input.

In the last stage of the workflow, different kinds of machine learning algorithms can be applied. This can include two potential pathways: one that exploits image asymmetry features and another one that uses images of segmented asymmetry. Machine learning classifiers, such as Naïve Bayes (NB), Linear Discriminant (LD), Support Vector Machines (SVMs) and K-Nearest Neighbor typically operate on the basis of feature vectors, such as image asymmetry features that can be used for training and testing. In contrast, a Deep Network (DN) classifier receives images of segmented asymmetry and generates its own features through training.

The data processing pipeline, including image processing and machine learning classification, has been implemented in Matlab using affordable and easy to obtain commodity hardware: Windows 10 Enterprise, processor – Intel (R) Core (TM), i7-7700 CPU@ 3.60GHz, 16 GB RAM.

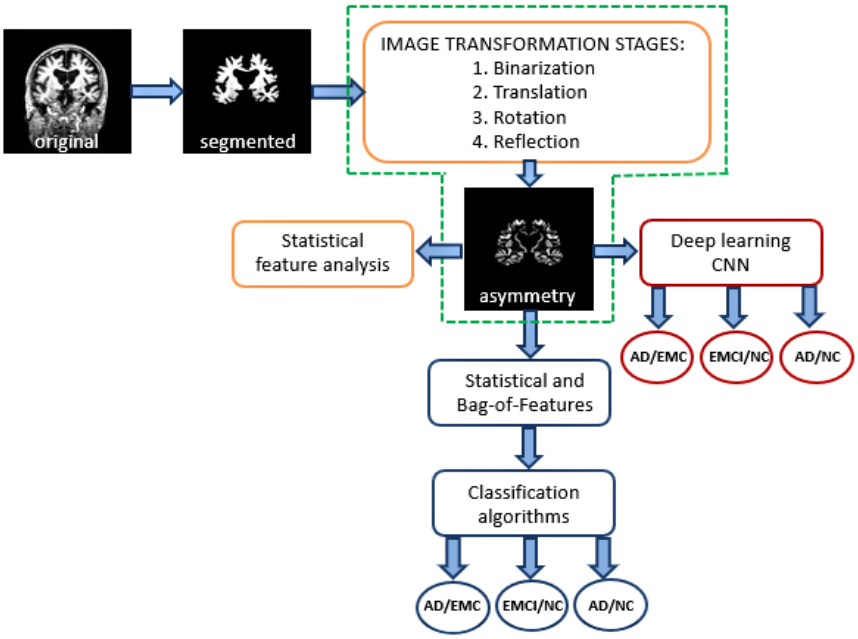

Fig.1 Machine learning workflow including image transformation stages, asymmetry features generation and machine learning classification algorithms

3.1 Image preprocessing and segmentation of image asymmetry

The preprocessing stage includes image normalization and image resizing procedures. All images are then segmented by implementing a brain segmentation algorithm with an adjusted threshold level of the pixel values (Fig. 2). Brain segmentation is an important task in the detailed study and analysis of the anatomical regions of the brain and their symmetries. It is often the most critical step in many medical applications. The manual segmentation step can be replaced with automatic segmentation software (AnalyzeDirect - https://analyzedirect.com/analyze14/, FreeSurfer - https://surfer.nmr.mgh.harvard.edu/, etc.).

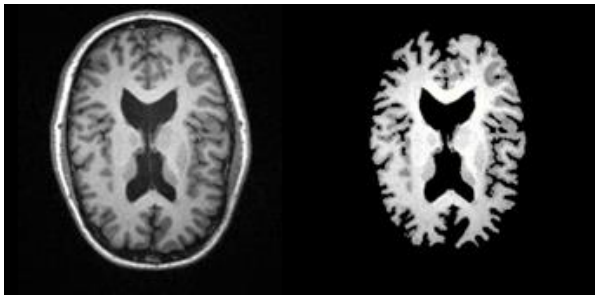

Fig.2 The segmentation of the brain tissues from the skull: original image (*left*), and segmented image of the brain (*right)*

There are many computer vision techniques proposed for the segmentation of specific brain areas in accordance with the anatomical atlas (Despotović et al. 2015). The current study presents an algorithm for the segmentation of the hemispheric asymmetries whose key point is the detection of the vertical axis of symmetry between the left and right hemispheres of the brain (Fig. 3). The hypothesis being tested in this part of the work is that there is an axis of reflective symmetry running through the center of the brain (Liu et al. 2001). The center point of the brain is allocated using an image binarization technique and calculating the image centroid (Teverovskiy and Li 2006). In the context of image processing and computer vision, the centroid is the weighted average of all the pixels in an image. The "weighted" centroid, or center of mass, is always at the exact center and depends on the gray levels in the image.

The technique of the allocation of an imaging center is accompanied by image binarization (Michalak and Okarma 2019), which converts a 256-shaded grayscale image to a binary (black and white-colored). The binarization is done according to the adjusted level of a threshold. All pixels in the image above the threshold level are replaced by the value 1 (white) and other pixels that are below that level, by the value 0 (black).

The brain center might differ from the center of the whole image including the background. If such a case occurs, the brain needs to be translated into the center of the image and rotated to the correct angle via the vertical axis. As soon as the brain centralization, translation, and rotation techniques are performed the image can be flipped or reversed from the left to the right across the vertical axis (Ruppert et al. 2011). The mirroring process is finalized by the segmentation of image asymmetries.

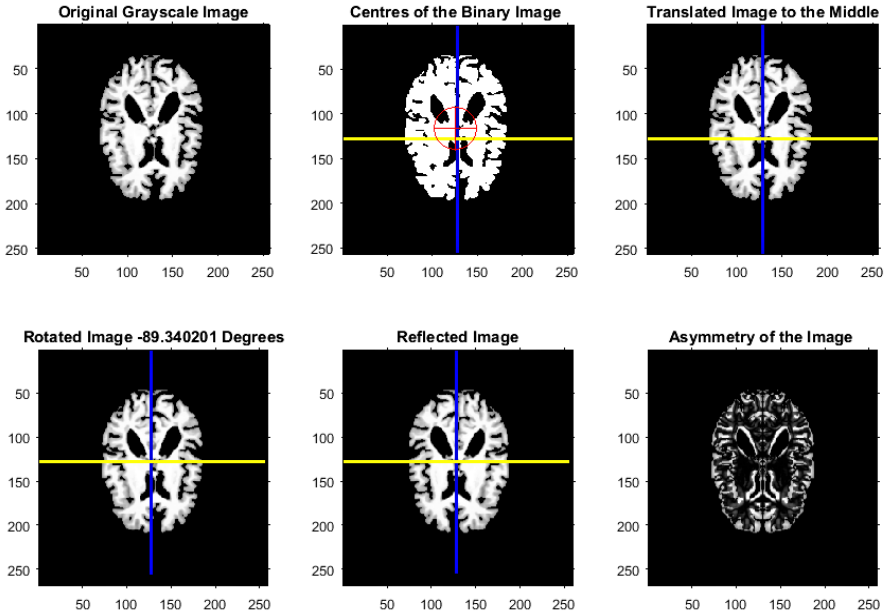

Fig.3 The image transformation stages for detection and segmentation of image asymmetries

The last image of this stage (see Fig. 3) is obtained as a result of mirroring of the left-brain hemisphere to the right and of the right-brain hemisphere to the left, which is followed by subtraction of the hemispheres from each other:

$$D = (L - R) + (R - L), \quad (1)$$

where D is an image asymmetry, L is an image matrix of the left hemisphere, R is an image matrix of the right hemisphere.

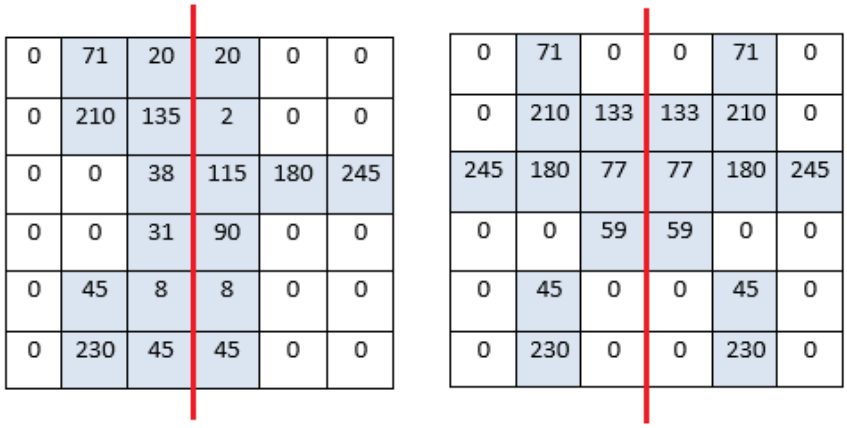

0	71	20	20	0	0
0	210	135	2	0	0
0	0	38	115	180	245
0	0	31	90	0	0
0	45	8	8	0	0
0	230	45	45	0	0

0	71	0	0	71	0
0	210	133	133	210	0
245	180	77	77	180	245
0	0	59	59	0	0
0	45	0	0	45	0
0	230	0	0	230	0

Fig.4 An illustrative example of matrix transformation values of a gray-scaled image of size 6-by-6: initial matrix (*left*) and Matrix of segmented asymmetry(*right*), mirrored via the vertical axis. The numbers in the cells correspond to the gray level of the pixel values

The symmetrical image areas (Fig. 4) get a value of 0 due to matrix subtraction. They are visualized as black areas in the image. The asymmetrical parts of the image are represented as different intensity gray levels from 1 to 255. The algorithm was tested on single slices of the brain, but the same idea can be extended and applied to the whole 3D brain image.

3.2 Feature engineering and analysis

Approaches that are based on statistical features for representing image properties are well-established in image processing (Di Ruberto and Fodde 2013). The statistical description of the image texture, color or morphological properties generates a limited number of relevant and distinguishable features. The proposed machine learning workflow uses ten strong and stable statistical features to represent the image asymmetries: MSE (Mean Squared Error), Mean, Std (Standard deviation), Entropy, RMS (Root Mean Square), Variance, Smoothness, Kurtosis, Skewness, IDM (Inverse difference moment). The first feature on the list, MSE, has been calculated directly from the original image and its mirrored version, while the rest of them are generated using discrete wavelet transform (DWT) as shown in Figure 5. In image processing, a discrete wavelet transform is a technique to transform image pixels into wavelets (Usman and Rajpoot 2017).

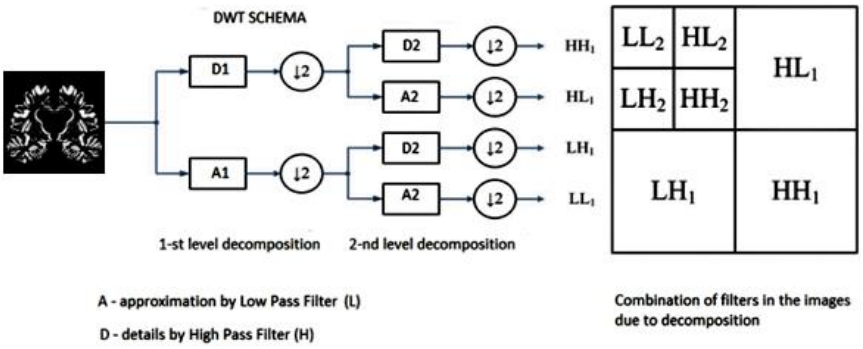

Fig.5 The DWT schema of the 1-st and the 2-nd level of the image decomposition after applying high- and low-pass filters in the horizontal and vertical directions

A brief description of each statistical feature used in this study is provided below.

3.2.1 Statistical features description

The features calculated from images or image asymmetries give information about the likelihood of gray pixel values in a random position in an image, their orientation, and interaction with other surrounding pixels. They are defined as follows:

Mean squared error (MSE)	The average squared intensity difference in the pixel values between the corresponding pixels of two images (Wang et al. 2004)
Mean	The texture feature that measures the average value of the intensity pixel values (Kumar and Gupta 2012); represents the brightness of the image.
Standard deviation (Std)	Shows the contrast of gray level intensities; indicates how much deviation or dispersion exists from the mean or average (Esmael et al. 2015).
Entropy	Entropy characterizes the image texture and measures the randomness of the pixel intensity distribution (Yang et al. 2012). It is the highest when all the pixel probabilities are equal.
Root mean square (RMS)	Measures the magnitude of a set of values (Lee et

	al. 2017); shows how far these values are from the line of best fit.
Variance	Measures the image heterogeneity (Yang et al. 2012); shows how the grayscale values differ from their mean.
Inverse difference moment (IDM)	Inverse difference moment (IDM) indicates the local homogeneity of an image (Yang et al. 2012); increases when pixel pairs are close in their grayscale values.
Smoothness	Smoothness measures the relative smoothness of intensity in an image (Malik and Baharudin 2013); it is high for an image region of constant intensity, and low for regions with large deviations in their intensity values.
Kurtosis	Measures the peak of the distribution of the intensity values around the mean (Ho and Yu 2015); often interpreted in combination with noise and resolution of the image (high kurtosis value is accompanied by low noise and low resolution).
Skewness	Shows the asymmetry of the probability distribution of the pixel intensity values about the mean value (Esmael et al. 2015); reveals information about image surfaces (darker and glossier surfaces tend to be more positively skewed than lighter and matte surfaces); any symmetric data have skewness near zero.

3.2.2 Analysis of image asymmetries

The analysis part is based on an evaluation of the statistical properties of segmented asymmetries.

Figure 6 shows averaging normalized (from 0 to 1) statistical data of each extracted feature from a set of 300 MRI slices of different patients with segmented asymmetries equally divided into three classes, those with Alzheimer's Disease - AD, Early Mild Cognitive Impairment - EMCI and Normal Cognitively - NC. Comparison of statistical features of AD, EMCI, and NC classes demonstrates the differences in their statistical characteristics.

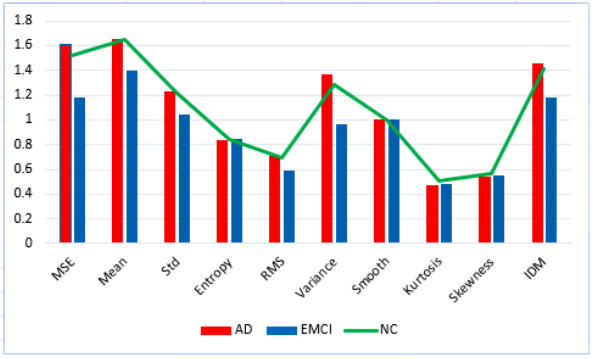

Fig.6 Red and blue bars correspond to the statistical mean of each image asymmetry feature for EMCI and AD patients: the green line shows how the AD and EMCI data differ from the NC patients

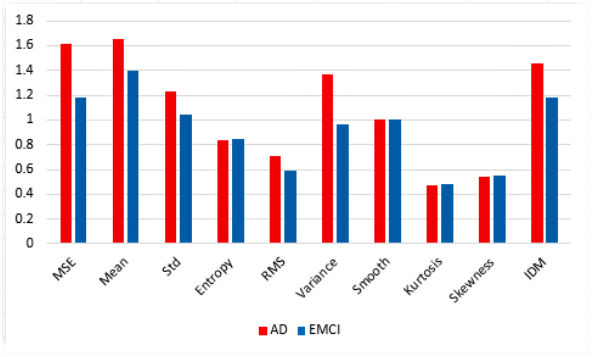

Fig.7 Statistical mean of asymmetry feature values for binary classes:
AD vs EMCI

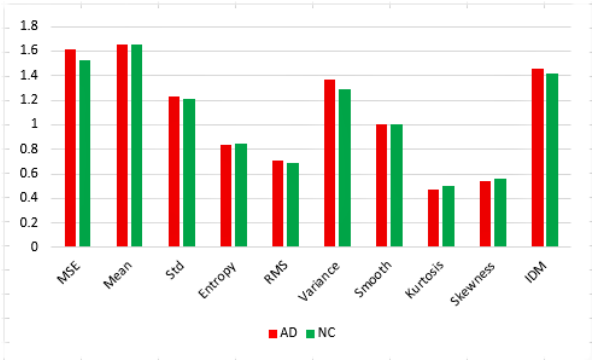

Fig.8 Statistical mean of asymmetry feature values for binary classes:
AD vs NC

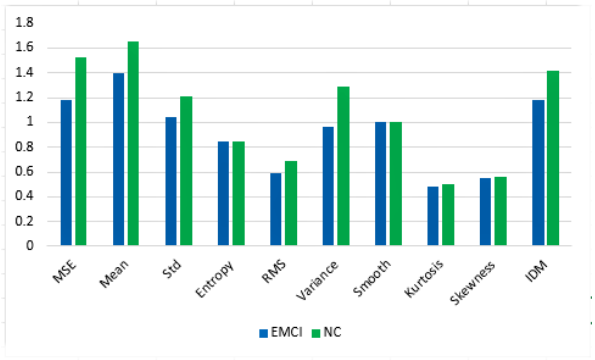

Fig.9 Statistical mean of asymmetry feature values for binary classes:
EMC vs NC

The highest difference between corresponding pixels of two images (MSE feature) belong to the AD class, the lowest result is shown for the EMCI class. The smallest averaging pixel intensity values, variance and standard deviation in the intensities are discovered in the EMCI class. These findings point to the relatively symmetrical object compared to those (AD and NC classes) which have noticeable pixel distribution values around the average. Pixels distribution values and probability around the mean demonstrate some sort of separation of the AD, EMCI and NC classes despite the amplitude of these values is less than registered with other statistical features. Texture features, such as entropy and IDM, prove the concept of variability between image classes. In this way, the features calculated the difference between original and inverted image matrices clearly indicate that EMCI data show more symmetry than NC and AD imaging data.

Figures 7-9 illustrate features comparison in three binary datasets: AD vs EMCI, AD vs NC, and EMCI vs NC. EMCI class demonstrates more symmetry than AD and NC classes in Figures 7 and 9. In Figure 8, statistical feature data of the AD class shows less symmetry than NC data.

The MSE feature analysis with a Pareto chart has been performed for male and female subjects (Figs. 10-11). The MSE value for each class has been calculated from the differences between the original image and its mirrored version for all images in classes of AD, EMCI, and NC.

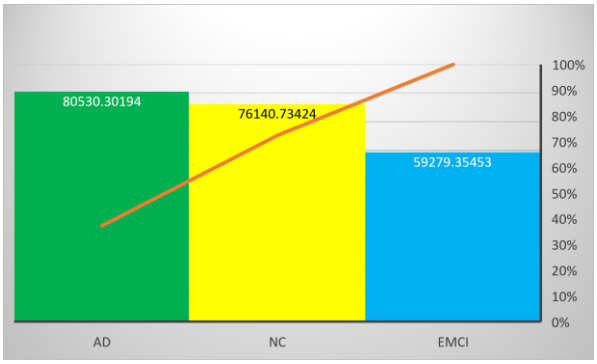

Fig.10 Pareto chart of MSE feature analysis for MRI slices of the male subject. The total MSE feature value is placed in the coloured bars. The axis, on the right, indicates the cumulative percentage of the total value for each class

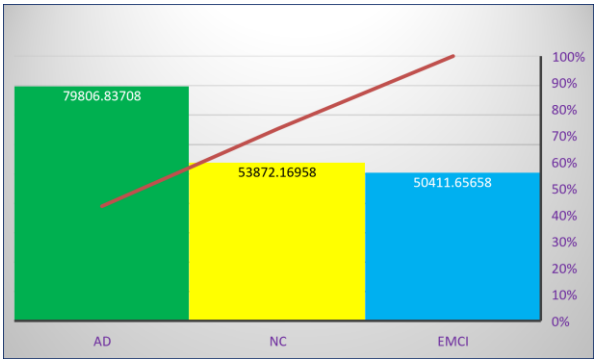

Fig.11 Pareto chart of MSE feature analysis for MRI slices of the female subject

The Pareto bar chart indicates the impact of asymmetry for each class. The highest MSE bar is associated with patients of the AD class. It confirms that changes in symmetry in the MRI slices of this image group are sizable compared to changes in the symmetry of other groups. At the same time, the EMCI image group has smaller values. The pattern of changes in male and female subjects does not show significant differences; nevertheless, the findings are consistent with the view that the female brain is more symmetrical than the male brain. The cumulative line of the secondary axis shows the contribution of each bar (image class) in the total value as a percentage.

A comparison of MSE values of 4 datasets is provided in Figure 12.

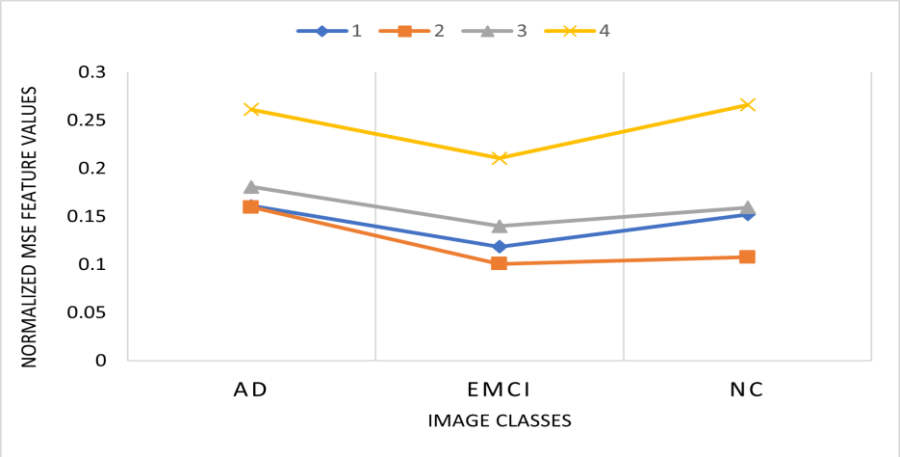

Fig.12 Comparison of MSE feature values between the three classes of MRIs. Numbers, 1,2…4, indicate the investigated datasets: #1 refers to a 150-image set of male MRIs in the coronal plane, #2 is a 150-image set of female MRIs in the coronal plane, #3 corresponds to a 300-images set of male subjects in the coronal plane, and #4 represents a 300-images set of males in the axial plane

Figure 12 illustrates the changes in MSE features between the three image classes, AD, EMCI and NC, in four completely different image sets. From the figure below, we can see the pattern of changes in the symmetry between the original and inverted images. The lowest MSE value for all image sets is obtained by images of the EMCI class.

The above analysis (Figs. 6-12) supports the view that image asymmetry decreases in the initial stage of the generative process in the brain (Early Mild Cognitive Impairment) and grows when the person develops moderate and severe dementia (Alzheimer's disease).

4 Experiments and Results

In this section, the two diagnostic pathways of the machine learning workflow are demonstrated and the robustness of brain asymmetry image and asymmetry features for early diagnosis of dementia is verified. To this end, SVMs and DNs are used, and the diagnosis problem is formulated as a set of binary classification problems.

T1-weighted MRIs of subjects aged between 55 and 75 years were used from the ADNI database. A total of 600 MRIs of brain asymmetries were generated, equally divided into groups of normal cognitively (NC) subjects, early mild cognitive impairment (EMCI) and Alzheimer's Disease (AD). MRIs were combined into 3 binary datasets: EMCI vs NC, AD vs NC and AD vs EMCI. The datasets consist of images of 2 dimensions (planes): vertical (frontal) and horizontal (axial). For the first diagnostic pathway, statistical features collected from image asymmetries were enriched with Bag-of-Features (BOF) to get the most detailed image "signatures" (Rueda et al. 2012). These were used to feed SVM classifiers with cubic and quadratic kernels (C-SVM and Q-SVM). The SVM performance was estimated using 10 simulation runs of a 10-fold cross-validation procedure and all models were tested on unseen data.

For the second diagnostic pathway (cf. Fig. 1), segmented brain asymmetry images were used, and features were generated as part of the training process of a Convolutional Neural Network (CNN)- a DN architecture that has shown in the literature very good performance in image classification tasks. To this end, transfer learning was used by adapting a well-known CNN, the so-called AlexNet (Krizhevsky et al. 2017). AlexNet has a total of 8 deep layers: five convolutional layers that are used for feature generations and three fully connected layers. The 1-st layer requires an input image of size 227-by-227-by-3, where 3 is the number of

color channels. The last 3 layers of AlexNet were preliminarily configured to 1000 classes as it was trained to solve a different classification problem, but they were replaced with a fully connected layer, a Softmax layer, and a binary classification output layer to fit the needs of the diagnosis tasks considered in this study (Fig. 13).

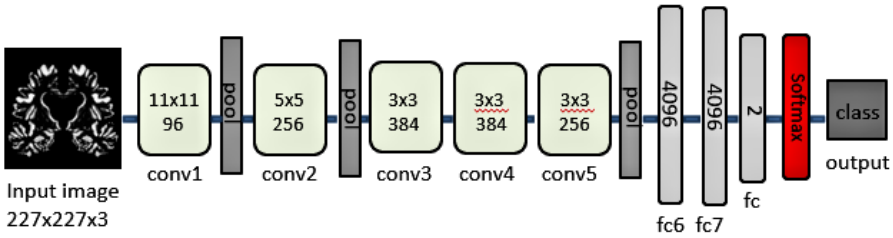

Fig.13 Adapted AlexNet architecture used in the experiments

The performance of the classification models was evaluated in terms of accuracy, sensitivity, specificity, and area under the curve (AUC) (Yang and Berdine 2017). The best available results obtained with the polynomial SVM classifier (C-SVM and Q-SVM) (Jakkula 2006) are shown in Table 3.

Table 3 Best available performance of Q-SVM and C-SVM in binary classification

Performance	EMCI vs NC		AD vs NC		AD vs EMCI	
	Q-SVM	C-SVM	Q-SVM	C-SVM	Q-SVM	C-SVM
Accuracy	0.93	0.93	0.93	0.95	0.87	0.86
Sensitivity	0.92	0.93	0.94	0.97	0.84	0.90
Specificity	0.94	0.93	0.92	0.93	0.90	0.82
AUC	0.97	0.98	0.97	0.99	0.94	0.94

The highest accuracy was achieved for the sets of EMCI vs NC, and AD vs NC. Based on the results, the detection of the EMCI in the early stage of the disease with quadratic and cubic SVMs gives an accuracy of 93%. These tests show a sensitivity of 92% and 93%, a specificity of 94% and 93%, and an AUC of 0.97 and 0.98 respectively. AD vs NC shows the highest performance equal to 95% of accuracy, 97% of sensitivity, 93% of specificity, and 0.99 of AUC for C-SVM.

To verify binary classification performance using brain asymmetry images, CNN parameters have been set as follows: 10 epochs, mini-batch size of 128, validation data frequency of 50. Before processing, the segmented asymmetry images were resized to 227×227×3 and fed into the model with 80% of the images used for training, 10% for validation, and 10% for testing. Table 4 summarises the best available result of the adapted AlexNet in the testing of the early mild cognitive impairment, normal cognitively, Alzheimer's disease datasets.

Table 4 Best available performance of CNN (adapted AlexNet) in binary classification

Performance	EMCI vs NC	AD vs NC	AD vs EMCI
Accuracy	0.76	0.90	0.82
Sensitivity	0.80	0.91	0.75
Specificity	0.72	0.89	0.89
AUC	0.90	0.92	0.88

Satisfactory performance with the CNN is obtained for all datasets by operating directly on images of segmented asymmetry without any feature engineering or fine-tuning prior to the classification. The average performance of CNNs in this problem is also promising as shown in (Herzog and Magoulas 2021) and one would expect that additional model optimization can improve the performance of CNNs further. This is a promising avenue for investigation, but it is considered out-of-scope for this chapter, and it will be the focus of our future work. The present study has verified the robustness and value of image asymmetries and demonstrated the operation of the machine learning workflow as a diagnostic tool when either image asymmetry features or segmented images of brain asymmetry are used.

5 Discussion and conclusion

Diagnosis based on an analysis of the changes in brain asymmetry opens a new possibility for the classification of mild cognitive impairment and Alzheimer's disease using MRI data. The chapter presented an approach for the analysis of brain asymmetries and the generation of image asymmetry features either by feature engineering or by learning segmented asymmetry MRI images. These find-

ings confirmed that changes in asymmetries convey important information about the progression of the disease. Thus, the segmented asymmetries can be beneficial for feature engineering and machine learning classification.

The proposed machine learning workflow offers a low-cost alternative for the classification of dementia as it does not require special hardware equipment. In contrast to other methods in the literature (see Section 2), the proposed image processing and feature engineering stages are less complex and take on average 0.1min per MRI image. This stage is not typically required when Deep Networks are applied since these models use the segmented MRI asymmetry slices directly as an input and can generate image features during network training.

Although optimizing the architecture of the machine learning algorithms can potentially increase performance, the accuracy of the models used in this study appears comparable with results obtained by more complex methods (see Section 2) for the ADNI database.

The proposed methodology has a perspective to explore the stages of Alzheimer's disease further. This research can be based on longitudinal studies of patient data. Changes in the shape of asymmetry and mapping these changes to the brain atlas will direct in those brain areas which are affected by the pathological process.

One more point for investigation is the comparison of asymmetries between the gray and white matter of the brain. Additional computer vision segmentation techniques might give a clue to the source of initial tissue deformation, which opens a direction for the early prediction and even prevention of the disease.

Acknowledgements: Data collection and sharing for this project was funded by the Alzheimer's Disease Neuroimaging Initiative (ADNI) (National Institutes of Health Grant U01 AG024904) and DOD ADNI (Department of Defense award number W81XWH-12-2-0012). ADNI is funded by the National Institute on Aging, the National Institute of Biomedical Imaging and Bioengineering, and through generous contributions from the following: AbbVie, Alzheimer's Association; Alzheimer's Drug Discovery Foundation; Araclon Biotech; BioClinica, Inc.; Biogen; Bristol-Myers Squibb Company; CereSpir, Inc.; Cogstate; Eisai Inc.; Elan Pharmaceuticals, Inc.; Eli Lilly and Company; EuroImmun; F. Hoffmann-La Roche Ltd. and its affiliated company Genentech, Inc.; Fujirebio; GE Healthcare; IXICO Ltd.; Janssen Alzheimer Immunotherapy Research & Develop-ment, LLC.; Johnson & Johnson Pharmaceutical Research & Development LLC.; Lumosity; Lundbeck; Merck & Co., Inc.; Meso Scale Diagnostics, LLC.; NeuroRx Research; Neurotrack Technologies; Novartis Pharmaceuticals Corporation; Pfizer Inc.; Piramal Imaging; Servier; Takeda Pharmaceutical Company; and Transition Therapeutics. The Canadian Institutes of Health Research is providing funds to support ADNI clinical sites in Canada. Private sector contributions are facilitated by the Foundation for the National Institutes of Health (www.fnih.org). The grantee organization is the Northern California Institute for Research and Education, and the study is coordinated by the Alzheimer's Therapeutic Research Institute at the

University of Southern California. ADNI data are disseminated by the Laboratory for Neuro Imaging at the University of Southern California.

References

Abdi H, Williams LJ (2010) Principal component analysis. Wiley interdisciplinary reviews: computational statistics 2(4):433-459

Agarwal M, Alam MR, Haider M et al (2021) Alzheimer's Disease: An Overview of Major Hypotheses and Therapeutic Options in Nanotechnology. Nanomaterials, 11(1), p.59

Basaia S, Agosta F, Wagner Let al (2019) Automated classification of Alzheimer's disease and mild cognitive impairment using a single MRI and deep neural networks. NeuroImage: Clinical, 21, p.101645

Beheshti I, Demirel H, Matsuda H et al (2017) Classification of Alzheimer's disease and prediction of mild cognitive impairment-to-Alzheimer's conversion from structural magnetic resource imaging using feature ranking and a genetic algorithm. Computers in biology and medicine 83: 109-119

Breiman, L (2001) Random forests. Machine learning 45(1):5-32

Bunge SA, Kahn I (2009) Cognition: An overview of neuroimaging techniques

Cabeza R, Daselaar SM, Dolcos F et al (2004) Task-independent and task-specific age effects on brain activity during working memory, visual attention and episodic retrieval. Cerebral cortex 14(4):364-375

Despotović I, Goossens B, Philips W (2015) MRI segmentation of the human brain: challenges, methods, and applications. Computational and mathematical methods in medicine, 2015

Di Ruberto C, Fodde G (2013) September. Evaluation of statistical features for medical image retrieval. In international conference on image analysis and processing, Springer, Berlin, Heidelberg, pp. 552-561

Ding S, Xu X, Nie R (2014) Extreme learning machine and its applications. Neural computing and applications 25(3):549-556

DSM-V (Diagnostic and statistical manual of mental disorders) 2013 updated https://www.psychiatry.org/psychiatrists/practice/dsm. Accessed 10 June 2020

Duchenne O, Bach F, Kweon IS et al (2011) A tensor-based algorithm for high-order graph matching. IEEE transactions on pattern analysis and machine intelligence 33(12):2383-2395

Esmael B, Arnaout A, Fruhwirth RK et al (2015) A statistical feature-based approach for operations recognition in drilling time series. International Journal of Computer Information Systems and Industrial Management Applications 5:454-61

Evgeniou T, Pontil M (1999) Support vector machines: Theory and applications. In advanced course on artificial intelligence. Springer, Berlin, Heidelberg, pp. 249-257 July 1999

Gainotti G (2019) The role of the right hemisphere in emotional and behavioral disorders of patients with frontotemporal lobar degeneration: an updated review. Frontiers in aging neuroscience, 11, p.55

Herzog N, Magoulas GD (2021) Deep learning of brain asymmetry images and transfer learning for early diagnosis of dementia. In international conference on engineering applications of neural networks, Springer, Cham, pp. 57-70 June 2021

Ho AD, Yu CC (2015) Descriptive statistics for modern test score distributions: Skewness, kurtosis, discreteness, and ceiling effects. Educational and Psychological Measurement 75(3):365-388

ICD-11 (International Classification of Diseases) for Alzheimer and Dementia 2018 released and endorsed in May 2019, https://icd.who.int/en. Accessed 27 January 2021.

Isles AR (2018) Epigenetics, chromatin and brain development and function. Brain and neuroscience advances 2:2398212818812011.

Jakkula V (2006) Tutorial on support vector machine (svm). School of EECS, Washington State University, 37

Janelidze M Botchorishvili N (2018) Mild cognitive impairment. Alzheimer's Disease: The 21st century challenge, 91

Johansen AM, Evers L, Whiteley N (2010) Monte carlo methods. Lecture notes, 200

Kim JH, Lee JW, Kim GH et al (2012) Cortical asymmetries in normal, mild cognitive impairment, and Alzheimer's disease. Neurobiology of aging 33(9):1959-1966

Kimberley TJ Lewis SM (2007) Understanding neuroimaging. Physical therapy 87(6):670-683

Krizhevsky A, Sutskever I, Hinton GE (2017) ImageNet classification with deep convolutional neural networks. Communications of the ACM 60(6)L:84-90

Kumar V, Gupta P (2012) Importance of statistical measures in digital image processing. International Journal of Emerging Technology and Advanced Engineering 2(8):56-62

Lama RK, Gwak J, Park JS et al (2017) Diagnosis of Alzheimer's disease based on structural MRI images using a regularized extreme learning machine and PCA features. Journal of healthcare engineering, 2017

Lee C, Zhang A, Yu B. et al (2017) Comparison study between RMS and edge detection image processing algorithms for a pulsed laser UWPI (Ultrasonic wave propagation imaging)-based NDT technique. Sensors 17(6):1224

Liu H, Zhang L, Xi Q et al (2018) Changes in brain lateralization in patients with mild cognitive impairment and Alzheimer's disease: A resting-state functional magnetic resonance study from Alzheimer's disease neuroimaging initiative. Frontiers in neurology, 9, p.3

Liu Y, Collins RT, Rothfus WE (2001) Robust midsagittal plane extraction from normal and pathological 3-D neuroradiology images. IEEE transactions on medical imaging 20(3):175-192

Malik F, Baharudin B (2013) The statistical quantized histogram texture features analysis for image retrieval based on median and Laplacian filters in the dct domain. The International Arab Journal of Information Technology 10(6):1-9

McManus C (2019) Half a century of handedness research: Myths, truths; fictions, facts; backwards, but mostly forwards. Brain and neuroscience advances 3:2398212818820513

Michalak H, Okarma K (2019) Improvement of image binarization methods using image preprocessing with local entropy filtering for alphanumerical character recognition purposes. entropy 21(6):562

Moradi E, Pepe A, Gaser C et al (2015) Machine learning framework for early MRI-based Alzheimer's conversion prediction in MCI subjects. Neuroimage 104:398-412

Nogueira J, Freitas S, Duro D (2018) Alzheimer's Disease Assessment Scale-Cognitive Subscale (ADAS-Cog): Normative Data for the Portuguese Population. Acta medica portuguesa 31(2):94-100

Pesarin F, Salmaso L (2010) The permutation testing approach: a review. Statistica 70(4):481-509

Robnik-Šikonja M, Kononenko I (2003) Theoretical and empirical analysis of ReliefF and RReliefF. Machine learning 53(1):23-69

Rueda A, Arevalo J, Cruz A et al (2012) Bag of features for automatic classification of Alzheimer's disease in magnetic resonance images. In iberoamerican congress on pattern recognition. Springer, Berlin, Heidelberg, pp. 559-566 September 2012

Ruppert GC, Teverovskiy L, Yu CP et al (2011) A new symmetry-based method for mid-sagittal plane extraction in neuroimages. In 2011 IEEE international symposium on biomedical imaging: from nano to macro. IEEE, pp. 285-288 March 2011

Segato A, Marzullo A, Calimeri F. et al (2020) Artificial intelligence for brain diseases: A systematic review. APL bioengineering 4(4):041503

Stamate D, Smith R, Tsygancov R et al. (2020) Applying deep learning to predicting dementia and mild cognitive impairment. In IFIP international conference on artificial intelligence applications and innovations. Springer, Cham, pp. 308-319 June 2020

Szaflarski JP, Rajagopal A, Altaye M (2012) Left-handedness and language lateralization in children. Brain research, 1433:85-97

Teverovskiy L, Li Y (2006) Truly 3D midsagittal plane extraction for robust neuroimage registration. In 3rd IEEE international symposium on biomedical imaging: nano to macro, IEEE pp. 860-863 April 2006

Tomasi D, Volkow ND (2012) Laterality patterns of brain functional connectivity: gender effects. Cerebral Cortex 22(6):1455-1462

Tripepi G, Jager KJ, Dekker FW et al (2008) Linear and logistic regression analysis. Kidney international 73(7): 806-810

Usman K, Rajpoot K (2017) Brain tumor classification from multi-modality MRI using wavelets and machine learning. Pattern analysis and applications 20(3):871-881

Wachinger C, Salat DH, Weiner M et al (2016) Whole-brain analysis reveals increased neuroanatomical asymmetries in dementia for hippocampus and amygdala. Brain 139(12):3253-3266

Wang Z, Bovik AC, Sheikh HR et al (2004) Image quality assessment: from error visibility to structural similarity. IEEE transactions on image processing 13(4):600-612

Welling M (2005) Fisher linear discriminant analysis, University of Toronto. Technical note

Wong DF, Maini A, Rousset OG et al (2003) Positron emission tomography: a tool for identifying the effects of alcohol dependence on the brain. Alcohol Research & Health 27(2):161

Yamashita R, Nishio M, Do RKG et al (2018) Convolutional neural networks: an overview and application in radiology. Insights into imaging 9(4):611-629

Yang C, Zhong S, Zhou X et al (2017) The abnormality of topological asymmetry between hemispheric brain white matter networks in Alzheimer's disease and mild cognitive impairment. Frontiers in aging neuroscience 9, p.261

Yang S, Berdine G (2017) The receiver operating characteristic (ROC) curve. The southwest respiratory and critical care chronicles 5(19):34-36

Yang X, Tridandapani S, Beitler JJ et al (2012) Ultrasound GLCM texture analysis of radiation-induced parotid-gland injury in head-and-neck cancer radiotherapy: An in vivo study of late toxicity. Medical physics 39(9): 5732-5739

Zhang D, Shen D (2012) Multi-modal multi-task learning for joint prediction of multiple regression and classification variables in Alzheimer's disease. NeuroImage 59(2):895-907

Zhu X, Suk HI, Wang L (2017) A novel relational regularization feature selection method for joint regression and classification in AD diagnosis. Medical image analysis 38:205-214